



Dual-responsive drug release and fluorescence imaging based on disulfide-pillar[4]arene aggregate in cancer cells

Mian Tang, Yao-Hua Liu, Xin-Miao Xu, Ying-Ming Zhang, Yu Liu

College of Chemistry, State Key Laboratory of Elemento-Organic Chemistry, Nankai University, Tianjin 300071, PR China

ARTICLE INFO

Keywords:

Supramolecular assemblies
Fluorescence tracing
Drug release
Tumor environment
Multistimuli-responsiveness

ABSTRACT

The construction of multistimuli-responsive nanoaggregate has become one of the increasingly significant research topics in supramolecular chemistry. We herein reported the pH- and glutathione dual-responsive supramolecular assemblies fabricated by the disulfide-containing pillar[4]arene and tetraphenylethylene derivatives possessing different alkyl chains in length. Morphological characterization experiments showed the binary supramolecular assemblies formed well-defined nanoparticles, which could facilitate their endocytosis in cells. More remarkably, due to the compact nanostructures and the existence of acidifiable carboxyl group and bioreducible disulfide linkage in pillar[4]arene, the obtained nanoaggregates presented high drug-loading efficiency and sustained drug release behaviors, as well as the targeted fluorescence imaging ability in cancer cells. Thus, it can be envisioned that such microenvironment-adaptable supramolecular nanoassemblies featuring dual stimuli-responsiveness and fluorescence-imaging abilities may be developed as more appealing nanosystems for the therapy of refractory disease.

1. Introduction

Despite the fact that numerous known and newly discovered molecules have exhibited great potentials for disease diagnoses and treatments, the lack of potent delivery carriers and desirable targeting abilities at the intended sites of action eventually leads them to the failure in clinical trials and application. To this end, the advent of macrocycle-based supramolecular chemistry has provided a sturdy tool to enhance biocompatibility and therapeutic efficacy of many hydrophobic drugs and bioactive molecules in a highly controllable manner.^{1–4} The dynamic and reversible characteristics of noncovalently chemical bonds can confer smart chemistry and stimuli-responsiveness to supramolecular nanoconstructs, which have been developed as a feasible approach to fabricate environmentally adaptable nanoassemblies for the treatments of many life-threatening diseases, such as cancers. In this context, due to their immense advantages of molecular recognition and robust assembly, supramolecular amphiphiles represent one of the most promising nanoassemblies with fascinating topological structures, including nanoparticles (NPs), vesicles, micelles, nanosheets, and nanorods.^{5–9} Consequently, considerable endeavors have been devoted to exploring their biological functions in drug delivery, biomedicines, and advanced therapeutics using various types of amphiphilic components, such as small molecules, macrocyclic receptors, and

polymeric macromolecules.^{10–12}

Compared to normal ones, there are many characteristics that are peculiar to malignant cells, which can be viewed as ideal biological stimuli and enable us to design more intelligent nanomedicines and implement more effective nanotherapeutics.¹³ For example, due to the overproduction of acidic metabolites in the process of glycolysis, the tumor environment is weakly acidic (≈ 6.5) than normal tissues (≈ 7.4), by which carboxylate anionic groups can be conveniently converted into carboxylic acids.^{14–16} Meanwhile, the dysfunction of glutathione (GSH) regulation can cause the overexpression of GSH in cancer cells, by which disulfide bonds can be selectively reduced to free thiols.^{17,18} Therefore, the synergistic combination of these intrinsic features of cancer cells, such as weakly acidic environment and high GSH concentration in tumor cells, can often be used to design advanced drug delivery systems.^{19,20}

In this work, by virtue of the naturally occurring biochemical stimuli in the cancer cells (i.e. low pH and bioreducing environment), two kinds of supramolecular amphiphiles were successfully constructed by the noncovalent communication between the water-soluble carboxylated cyclic tetramer possessing disulfide bonds (**1**)^{21–23} and the quaternary ammonium salts possessing tetraphenylethylene (TPE) group (TPENC_n, n = 6 and 12).^{24–27} Benefiting from the acidifiable carboxylate groups and the reduction-sensitive disulfide bonds in **1**, specific disaggregation

E-mail addresses: ymzhang@nankai.edu.cn (Y.-M. Zhang), yuliu@nankai.edu.cn (Y. Liu).

<https://doi.org/10.1016/j.bmc.2022.116649>

Received 5 December 2021; Received in revised form 12 January 2022; Accepted 26 January 2022

Available online 2 February 2022

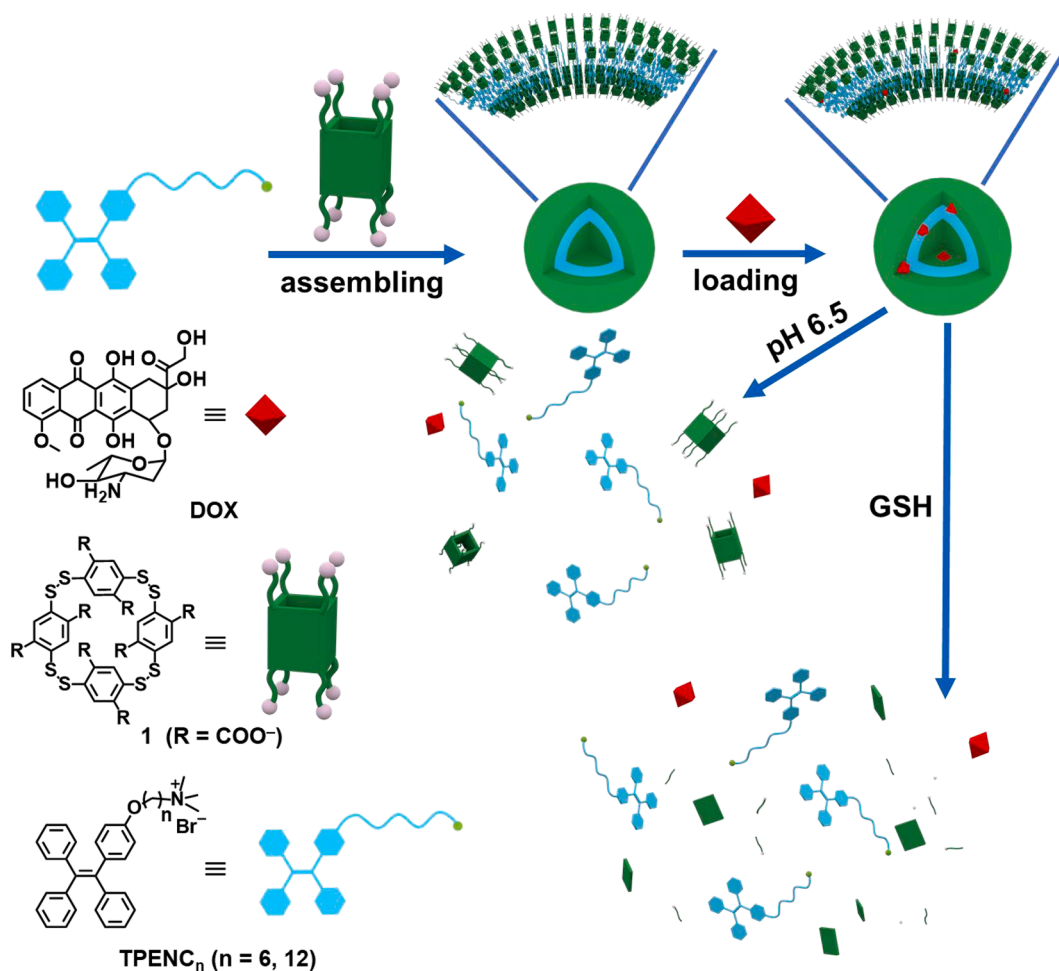
0968-0896/© 2022 Elsevier Ltd. All rights reserved.

of the obtained amphiphilic nanoassemblies and the concomitant drug release could be concurrently achieved in response to the slightly acidic and GSH-overexpressed microenvironment inside the cancer cells. More interestingly, strong fluorescence emission was realized in the intact supramolecular amphiphiles through the aggregation-induced emission (AIE) pathway. Comparatively, the fluorescence emission could be seriously weakened as soon as the amphiphilic superstructures were disrupted, thus realizing in-situ monitoring of drug delivery and release process in both inanimate milieu and cancer cells. Hence, this study not only demonstrates the superiority of multistimuli-responsive supramolecular amphiphiles in the targeted delivery of therapeutic agents but also manifests that the assembly-enhanced photoluminescence can be utilized as a feasible method in monitoring the drug release process.^{28–32}

2. Results and discussion

The construction of supramolecular TPENC_n@1 (n = 6 and 12) amphiphiles and their multistimuli-responsive drug delivery of doxorubicin (DOX) are depicted in Scheme 1. The negatively charged disulfide-containing pillar[4]arene **1** could bind to the positively charged TPENC_n through multiple electrostatic interactions. The carboxylate anionic groups of **1** and the quaternary ammonium sites of TPENC_n served as the hydrophilic parts, while the aromatic backbones of **1** and TPENC_n served as the hydrophobic parts. The assembly-induced aggregation between **1** and TPENC_n could readily form amphiphilic supramolecular NPs by lowering the critical aggregation concentration (CAC) of TPENC_n.³³ For example, no aggregation was observed for free

TPENC₆ below 100 μM (Figs. 1 a–b and S11–S12), whereas the CAC value sharply decreased in the presence of **1** at 5 μM (Fig. 1a). The molecular assembling properties of TPENC_n with **1** were further confirmed by the changes in optical transmittance, which is a reliable characterization method to evaluate the formation of amphiphilic assemblies. In our case, no obvious change of optical transmittance was observed in the TPENC_n alone; however, the optical transmittance at 650 nm dramatically decreased upon increasing the concentration of TPENC_n, and the appearance of points of inflection indicated the formation of large-sized aggregates in solution.³⁴ Meanwhile, no turbidity or precipitation was observed under our experimental condition. Accordingly, the CAC values of TPENC₆@1 and TPENC₁₂@1 were obtained as 36.9 and 41.8 μM, respectively (Figs. 1b and S13). Moreover, when the concentration of **1** was fixed, it is found that the optimal molar ratios of TPENC₆@1 and TPENC₁₂@1 were determined as 5:1 and 6:1 respectively (Figs. S14 and S15). The bulky TPE group could impede the quaternary ammonium head of TPENC_n from the efficient electrostatic attraction with the carboxylate anionic group of tetramer **1**, which is contributed to the optimal mixing ratios unequally available to the charge ratio (8:1). In addition, the hexyl-bearing quaternary ammonium salt (NC₆) was chosen as the reference to check if there is any host-guest interaction between TPENC_n and **1**. Although the proton peaks of NC₆ were passivated upon addition of **1** in the ¹H NMR spectrum, no correlation peak was observed by means of rotating-frame Overhauser effect spectroscopy (ROESY, Figs. S16 and S17). Therefore, no obvious host-guest interaction is involved but electrostatic attraction is believed as the main driving force in the formation of these supramolecular amphiphiles.



Scheme 1. Schematic illustration of the assembling and disassembling of the DOX-loaded TPENC_n@1 (n = 6 and 12) supramolecular amphiphiles in response to acidic environment and over-expressed GSH. The green squares are denoted as the decomposed **1** after reduction by GSH.

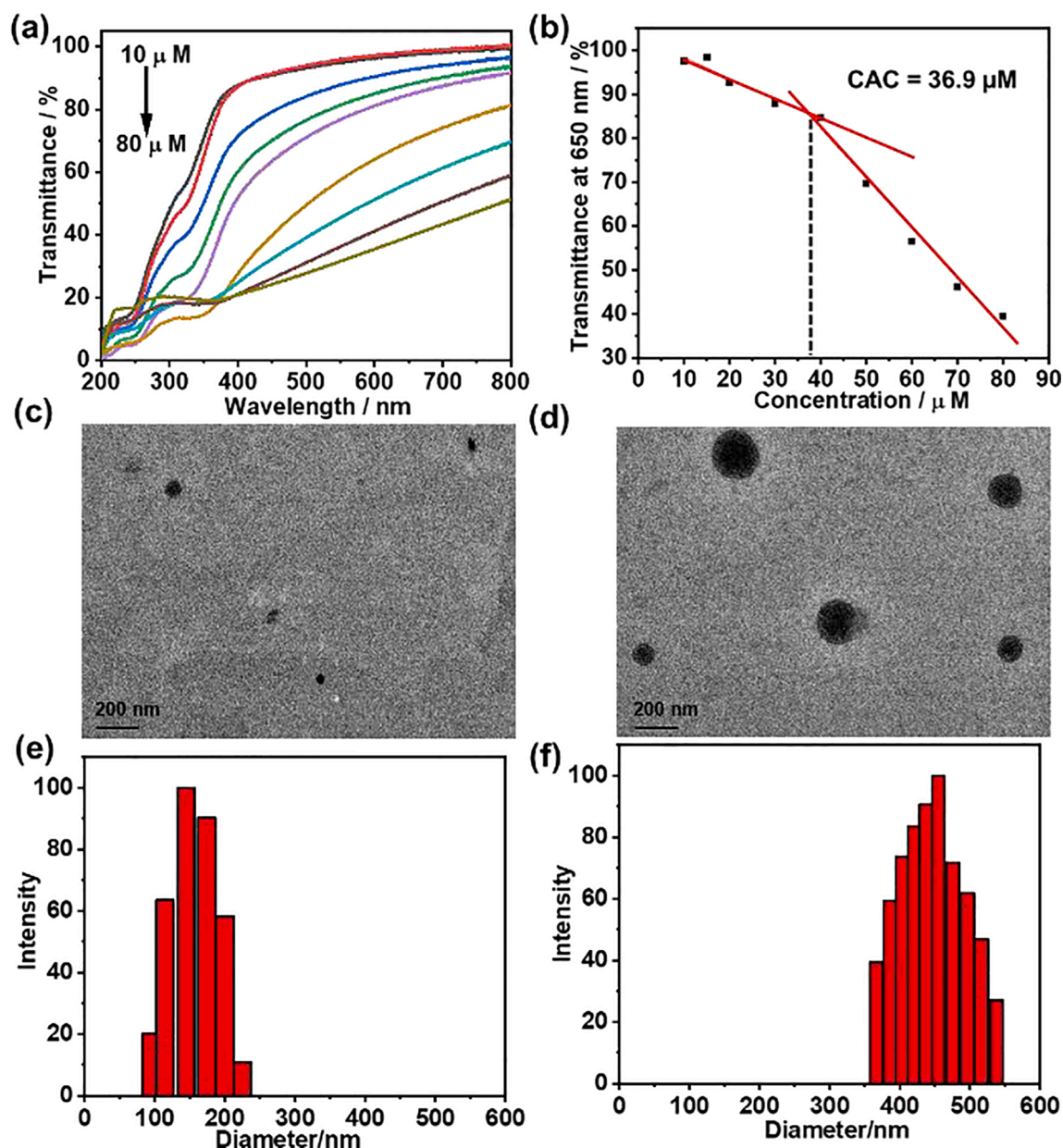


Fig. 1. (a) Optical transmittance of **1** (20 μM) with TPENC₆ at different concentrations in PBS (pH = 7.2) at 25 °C. (b) Dependence of the optical transmittance at 650 nm on the TPENC₆ concentration in the presence of **1** (20 μM) in PBS (pH = 7.2) at 25 °C. DLS data and TEM images of (c, e) free TPENC₆ and (d, f) TPENC₆@**1** assembly.

Furthermore, the transmission electron microscopic (TEM) images showed that the sizes of free TPENC₆ and TPENC₁₂ were obtained as 25 and 30 nm, respectively (Figs. 1c and S18). In comparison, the aggregation of TPENC₆@**1** and TPENC₁₂@**1** gave large-sized NPs with diameters of ca. 100 and 460 nm, respectively (Figs. 1d and S19). The spherical aggregates of TPENC_n@**1** could be classified as a type of supramolecular NPs, since there was no definite evidence to prove whether they were hollow or solid. Nevertheless, the suitable assembling sizes may facilitate their endocytosed into cells. Meanwhile, the dynamic light scattering (DLS) data also showed that the average hydrodynamic diameters increased to 455 and 1041 nm when TPENC₆ and TPENC₁₂ were mixed with **1** in aqueous solution, respectively (Figs. 1e–f and S20–S21). The relatively larger sizes obtained in the DLS experiments are reasonable, because the contribution of hydrodynamic diameter should be considered in aqueous environment. Based on these observations, a reasonable self-assembling mechanism on the formation of supramolecular NPs may be elucidated as follows: free TPENC_n cannot

spontaneously aggregate into large-sized nanoassemblies at lower concentration. Comparatively, upon addition of tetramer **1**, one **1** and several TPENC_n molecules formed multi-layered and well-defined aggregates with an alternating shell structure arising from the multiple electrostatic and hydrophobic interactions.

Subsequently, the stimuli-responsive properties of these obtained amphiphiles were studied. Owing to the acidifiable carboxylate anion group and cleavable disulfide linkage, the disulfide-containing pillar[4] arene **1** could undergo structural transformation in the acidic and reducing environments, which would eventually lead to the specific disaggregation of supramolecular NPs. As discerned from Fig. 2a, when the pH value was adjusted to 6.5 or excess GSH was added into the solution of supramolecular NPs, the optical transmittance increased to a great extent (Fig. 2a). Indeed, it is shown that 17.8% of tetramer **1** was protonated at pH = 6.5 by potentiometric titration (Fig. S22). In addition, no obvious fluorescence emission was observed in the dilute solution of free TPENC₆. However, the addition of **1** could efficiently induce the

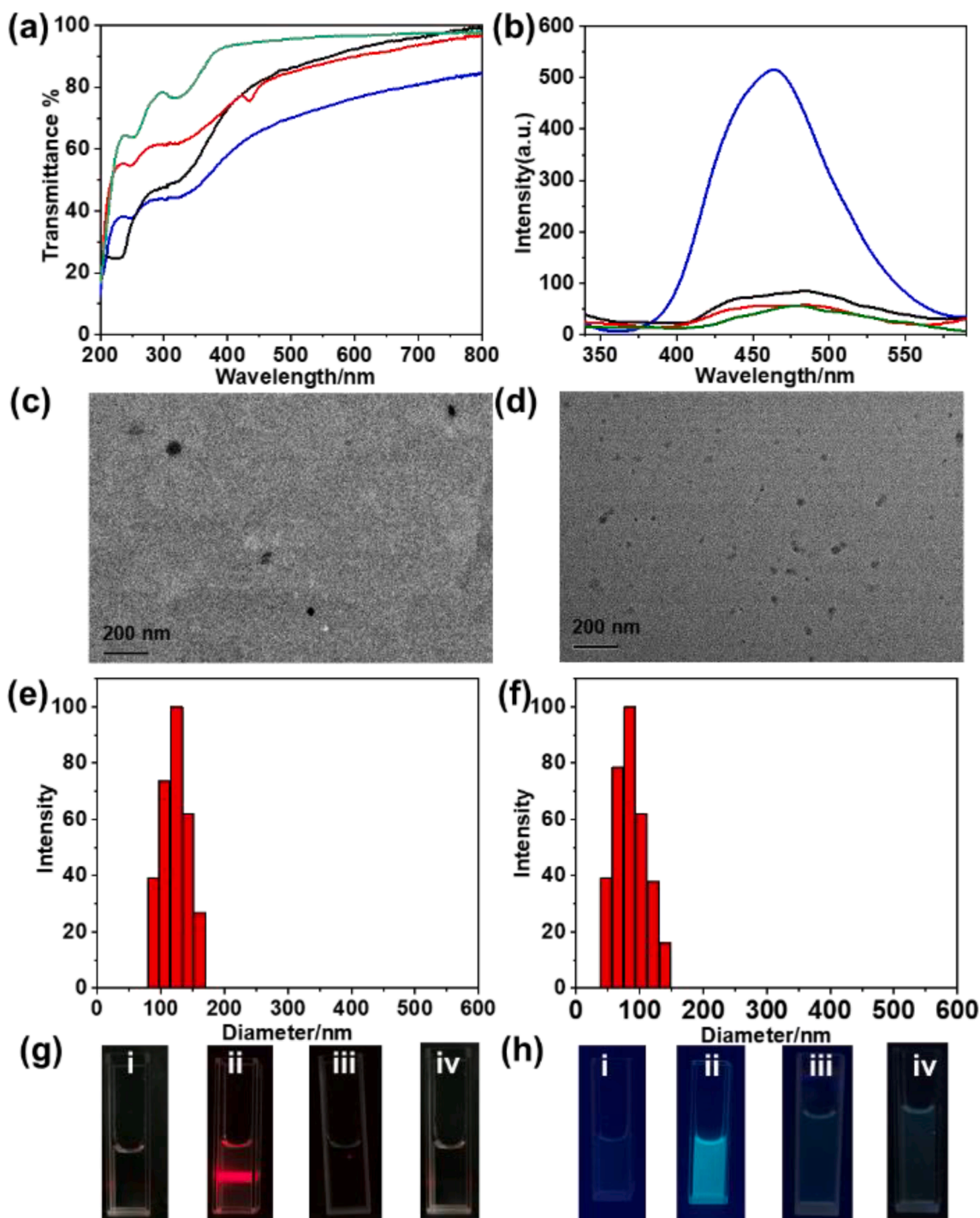


Fig. 2. (a) Optical transmittance of TPENC₆ (green line), TPENC₆@1 (blue line), TPENC₆@1 + GSH (black line) in PBS (pH = 7.2) and TPENC₆@1 (pH = 6.5) in water (red line) at 25 °C ([TPENC₆] = 30 μM, [1] = 5 μM, and [GSH] = 200 μM); (b) Fluorescence emission spectra of TPENC₆ (green line), TPENC₆@1 (blue line), TPENC₆@1 + GSH (black line) in PBS (pH = 7.2), and TPENC₆@1 at pH = 6.5 in water (red line) at 25 °C ([TPENC₆] = 30 μM, [1] = 5 μM, and [GSH] = 200 μM, λ_{ex} = 330 nm). TEM images and DLS data of (c, e) TPENC₆@1 + GSH and (d, f) TPENC₆@1 at pH = 6.5; (g) The Tyndall effect and (h) photographs of (i) TPENC₆, (ii) TPENC₆@1, (iii) TPENC₆@1 + GSH, and (iv) TPENC₆@1 (pH = 6.5) under light irradiation at 365 nm.

aggregation of TPENC₆ in a compact form, thus achieving its typical fluorescence emission of TPE core centered at 460 nm in PBS (Fig. 2b). In contrast, under the weakly acidic and reducing condition, the fluorescence emission was seriously quenched, accompanied by the reappearance of small-sized NPs in the TEM images and DLS data (Fig. 2c–f). Only the TPENC₆@1 group gave an obvious Tyndall effect and strong blue-green fluorescence emission under the light irradiation, which could be conveniently observed by the naked eyes (Fig. 2g and h).

Similar experimental observations were obtained using TPENC₁₂ (Figs. S23–S28). As discerned from Fig. S24, TPENC₁₂ alone showed distinct fluorescence emission at 475 nm, due to the strong tendency of self-aggregation with long hydrophobic alkyl chain. As a result, compared to TPENC₁₂@1 NPs, more remarkable fluorescence emission enhancement was observed in the case of TPENC₆@1. Thus, benefiting from the favorable noncovalent interactions, the aggregation of TPENC_n can be greatly promoted with assistance of 1 and more importantly, the

dissociation of supramolecular NPs can be achieved with desirable pH- and redox-responsive capabilities. With the dual responsive supramolecular amphiphiles in hand, their drug loading and release behaviors were explored using DOX as the drug model, because DOX can be readily located at the hydrophobic region of the TPENC_n@1 NPs. The drug encapsulation and loading efficiencies were calculated as 36.4% and 4.9% for TPENC₆@1 and 32.4% and 4.3% for TPENC₁₂@1, respectively (Figs. 3a–b and S29–S32).^{35,36} Moreover, the drug release behaviors of TPENC₆@1 *in vitro* were also investigated. By comparing the drug release profiles under different conditions, it is found that only 35.3% DOX was released from the binary supramolecular NPs in the neutral solution, whereas the release rates were dramatically accelerated and more drugs were released under the acidic or GSH-expressed condition in 6 h. More gratifyingly, DOX could be completely released when acid and GSH co-existed in the solution of TPENC₆@1 in the same period of time (Fig. 3c and d). The UV–vis absorption spectral changes versus time were recorded in Figs. S33 and S34. Apparently, these obtained supramolecular amphiphiles possessed good drug encapsulation, loading efficiencies, and desired multi-stimuli responsiveness toward redox and pH changes, which would facilitate the controlled and targeted drug delivery and release in the cancer cells, as described below.

Given the more suitable assembling size, better stimuli-responsive characteristics, and relatively higher drug-loading capacity, the drug release behaviors of TPENC₆@1 NPs were investigated toward the

normal and cancer cells. Due to the microenvironment of cancer cells, the supramolecular amphiphiles could readily lead the rapid drug release of DOX in the cancer cells (A549 cell line). Bright red fluorescence arising from the released DOX and faint blue-green fluorescence arising from the disaggregated TPENC₆ could be observed. In contrast, in the normal cells (293T cell line), the obtained supramolecular amphiphiles maintained their integrity and no drug could escape from the compact NPs. Therefore, the bright red fluorescence of DOX and the strong blue-green fluorescence of TPENC₆ could be observed at the same time and they had good overlap with each other in a single cell (Figs. 4a and S35). Moreover, the toxicity of the supramolecular NPs was tested. As can be seen from Fig. 4b and c, the drug-free NPs showed no significant cytotoxicity for both cells, but only the DOX-loaded ones could dramatically reduce the viability of cancer cells. In comparison, DOX alone did not show significant cytotoxicity, probably due to the relatively shorter incubation time in our case. Meanwhile, supramolecular nanodrugs are known to possess improved abilities of internalization and accumulation in cells compared to the parent drugs at the same dose.³⁷ Accordingly, the half-maximal inhibitory concentration (IC₅₀) of the DOX-loaded NPs was calculated as 4.2 μg/mL for the A549 cells. Similar cell-targeting ability was also observed by using BEAS-2B cells as the normal control (Fig. S36). These experimental results jointly demonstrate that benefitting from the characteristic environments in cancer cells, our obtained NPs could specifically delivery and release

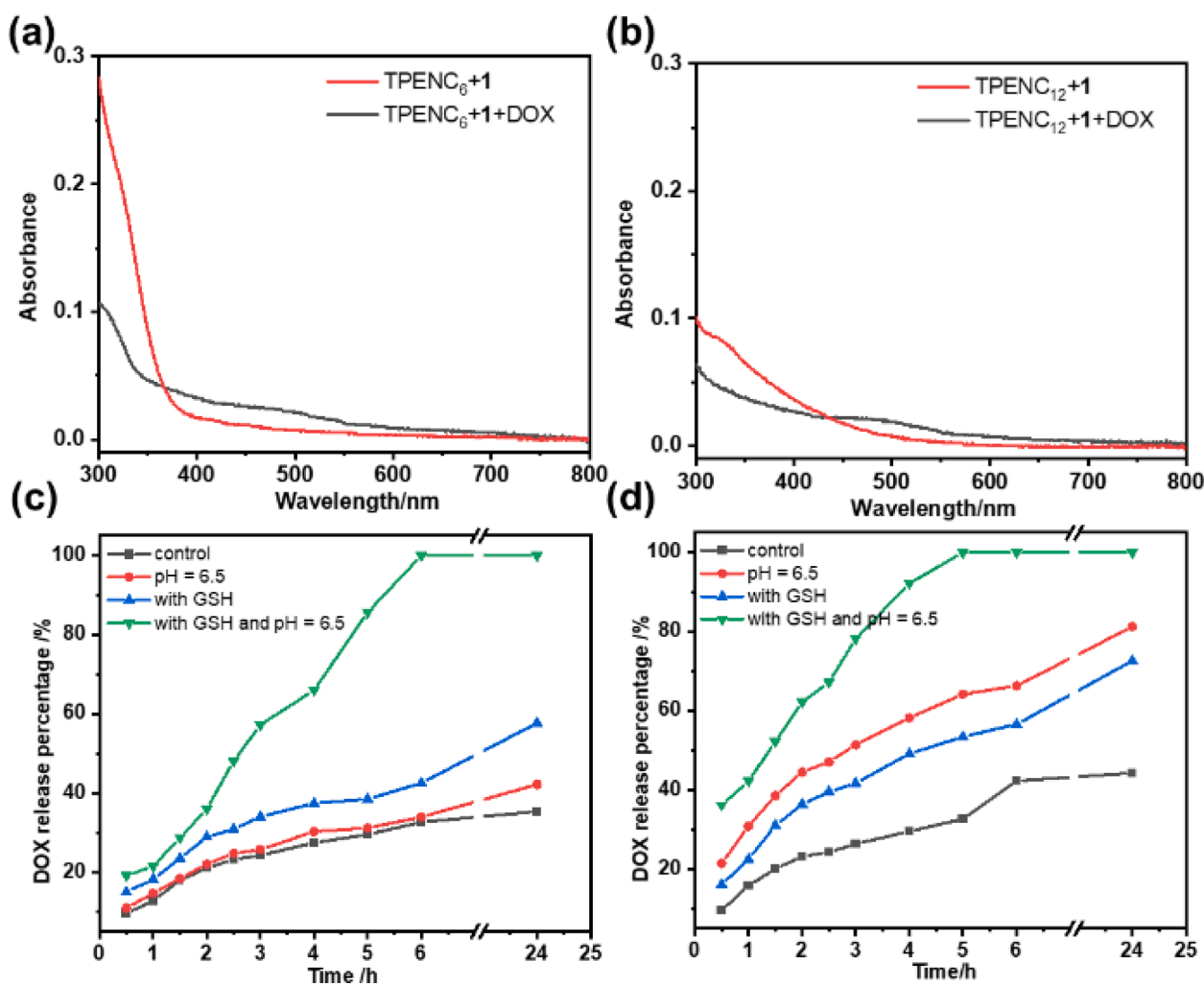


Fig. 3. UV–vis absorption spectra of (a) TPENC₆@1 NPs and (b) TPENC₁₂@1 NPs before and after loading DOX. *In vitro* release profiles of DOX by (c) drug-loaded TPENC₆@1 NPs and (d) drug-loaded TPENC₁₂@1 NPs in the absence of GSH in PBS (pH = 7.2) (black line), in the presence of GSH in PBS (pH = 7.2) (blue line), in the acidic aqueous solution (pH = 6.5) (red line) and acid and GSH co-existed (green line) in the aqueous solution at 25 °C.

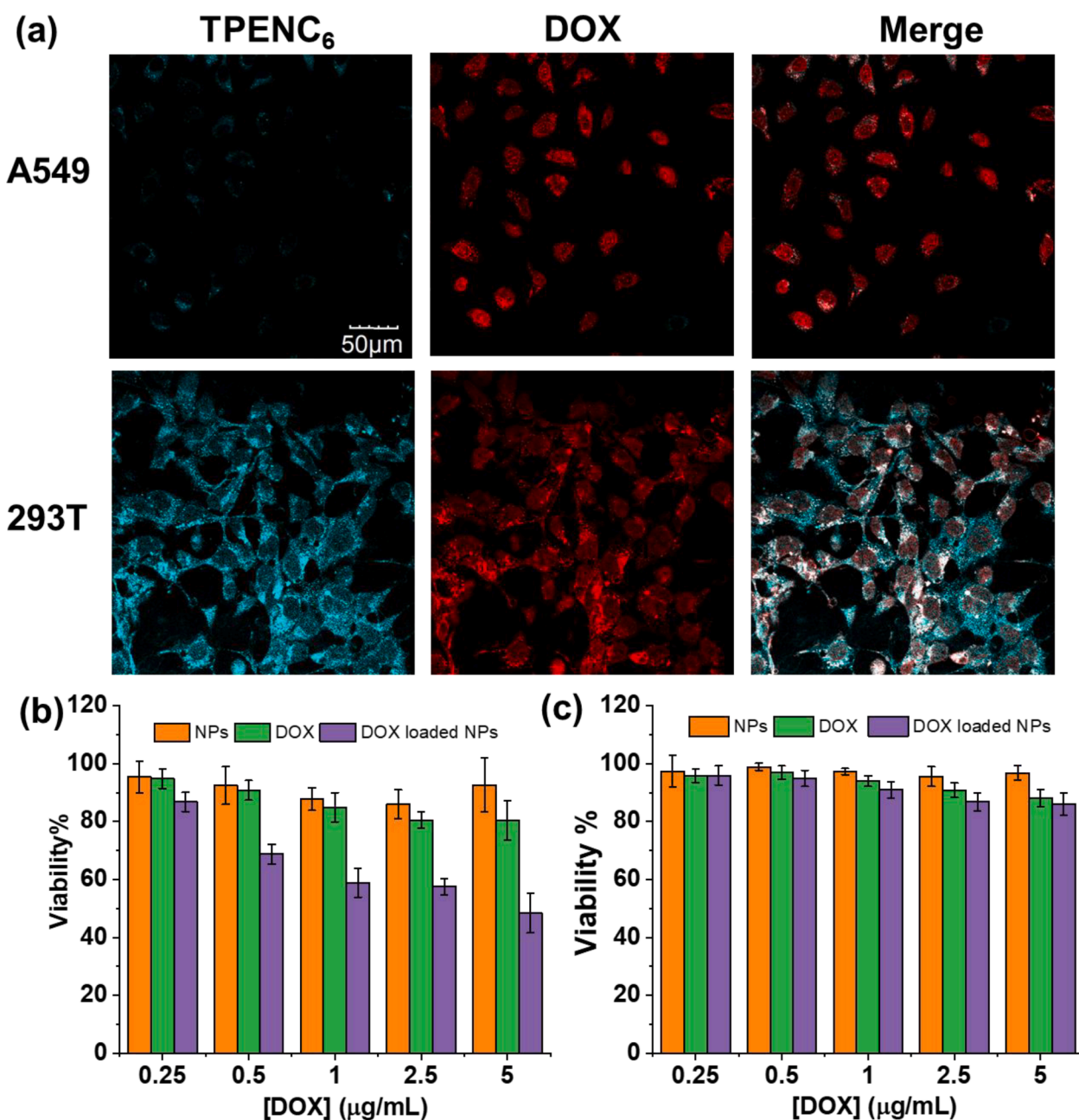


Fig. 4. (a) Confocal microscopic images of A549 and 293T cells after incubation with DOX-loaded TPENC₆@1 NPs for 12 h ([DOX] = 5 μg mL⁻¹). Relative cellular viabilities of (b) A549 and (c) 293T cells after the treatment with free and DOX-loaded TPENC₆@1 NPs, respectively, after incubation in 24 h.

anti-cancer drugs into cancer cells but cause no adverse effect toward normal cells. Meanwhile, the drug release process could be conveniently monitored by the changes of fluorescence emission intensity of nanocarriers.

3. Conclusions

In conclusion, two supramolecular amphiphiles were successfully constructed by the multiple noncovalent interactions between the disulfide-pillar[4]arene (1) and tetraphenylethylene (TPE) derivatives containing quaternary ammonium salts, which showed dual pH- and redox-responsive drug release behaviours. Co-assembly of 1 and TPENC₆ formed supramolecular NPs in neutral solution and exhibited blue-green fluorescence at 478 nm via the characteristic AIE pathway. The anti-cancer drug DOX loaded in the binary TPENC₆@1 supramolecular NPs could be specifically and rapidly released in the cancer cells due to their

mild acidic and over-expressed GSH environments. More significantly, it is also found that the drug release process was highly associated with the disaggregation of supramolecular NPs and the decrease in fluorescence emission intensity. To be envisioned, the advanced drug loading and delivery efficiency combined with the in-situ monitoring of drug release can eventually lead to the potent chemotherapy for dramatically inhibiting tumor growth, thus demonstrating our tumor microenvironment-adaptable nanosystems as new promising candidates for oncological treatments in the future.

Declaration of Competing Interest

The authors declare that they have no known competing financial interests or personal relationships that could have appeared to influence the work reported in this paper.

Acknowledgments

We thank Dr. Yuanyuan Hou at College of Pharmacy (Nankai University) for providing BEAS-2B cells. This work was financially funded by the National Natural Science Foundation of China (grants 21871154, 22171148, and 22131008) and the Fundamental Research Funds for the Central Universities, Nankai University.

Appendix A. Supplementary material

Supplementary data to this article can be found online at <https://doi.org/10.1016/j.bmc.2022.116649>.

References

- [1] Xing P, Zhao Y. Supramolecular Vesicles for Stimulus-Responsive Drug Delivery. *Small Methods*. 2018;2:1700364.
- [2] Kim E, Kim D, Jung H, et al. Facile, Template-Free Synthesis of Stimuli-Responsive Polymer Nanocapsules for Targeted Drug Delivery. *Angew. Chem. Int. Ed.* 2010;49:4405–4408.
- [3] Wu M-X, Yang Y-W. Metal-Organic Framework (MOF)-Based Drug/Cargo Delivery and Cancer Therapy. *Adv. Mater.* 2017;29:1606134.
- [4] Yang J, Yang Y-W. Metal-Organic Frameworks for Biomedical Applications. *Small*. 2020;16:1906846.
- [5] Wang C, Wang Z, Zhang X. Amphiphilic Building Blocks for Self-Assembly: From Amphiphiles to Supra-amphiphiles. *Acc. Chem. Res.* 2012;45:608–618.
- [6] Park KM, Hur MY, Ghosh SK, Boraste DR, Kim S, Kim K. Cucurbit[n]uril-Based Amphiphiles That Self-Assemble into Functional Nanomaterials for Therapeutics. *Chem. Commun.* 2019;55:10654–10664.
- [7] Li Z, Song N, Yang Y-W. Stimuli-Responsive Drug-Delivery Systems Based on Supramolecular Nanovalves. *Matter*. 2019;1:345–368.
- [8] Yue L, Yang K, Lou X-Y, Yang Y-W, Wang R. Versatile Roles of Macrocycles in Organic-Inorganic Hybrid Materials for Biomedical Applications. *Matter*. 2020;3:1557–1588.
- [9] Song N, Lou X-Y, Ma L, Gao H, Yang Y-W. Supramolecular Nanotheranostics Based on Pillararenes. *Theranostics*. 2019;9:3075–3093.
- [10] Jie K, Zhou Y, Yao Y, Huang F. Macrocyclic amphiphiles. *Chem. Soc. Rev.* 2015;44:3568–3587.
- [11] Chang Y, Jiao Y, Symons HE, Xu J-F, Faul CFJ, Zhang X. Molecular Engineering of Polymeric Supra-amphiphiles. *Chem. Soc. Rev.* 2019;48:989–1003.
- [12] Zheng Z, Geng W-C, Xu Z, Guo D-S. Macrocyclic Amphiphiles for Drug Delivery. *Isr. J. Chem.* 2019;59:913–927.
- [13] Liu Y-H, Zhang Y-M, Yu H-J, Liu Y. Cucurbituril-Based Biomacromolecular Assemblies. *Angew. Chem.* 2021;60:3870–3880.
- [14] Liu G, Zhao X, Zhang Y, et al. Engineering Biomimetic Platemers for pH-Responsive Drug Delivery and Enhanced Antitumor Activity. *Adv. Mater.* 2019;31:1900795.
- [15] Gong Y, Chen H, Ma X, Tian H. A Cucurbit[7]uril Based Molecular Shuttle Encoded by Visible Room-Temperature Phosphorescence. *ChemPhysChem*. 2016;17:1934–1938.
- [16] Shi B, Jie K, Zhou Y, Zhou J, Xia D, Huang F. Nanoparticles with Near-Infrared Emission Enhanced by Pillararene-Based Molecular Recognition in Water. *J. Am. Chem. Soc.* 2016;138:80–83.
- [17] Liu Z, Zhou X, Miao Y, et al. A Reversible Fluorescent Probe for Real-Time Quantitative Monitoring of Cellular Glutathione. *Angew. Chem. Int. Ed.* 2017;56:5812–5816.
- [18] Umezawa K, Yoshida M, Kamiya M, Yamasoba T, Urano Y. Rational Design of Reversible Fluorescent Probes for Live-cell Imaging and Quantification of Fast Glutathione Dynamics. *Nat. Chem.* 2017;9:279–286.
- [19] Liang K, Sun H, Yang Z, et al. Breaking the Redox Homeostasis: an Albumin-Based Multifunctional Nanoagent for GSH Depletion-Assisted Chemo-/Chemodynamic Combination Therapy. *Adv. Funct. Mater.* 2021;31:2100355.
- [20] Yang Z, Fan W, Tang W, et al. Near-Infrared Semiconducting Polymer Brush and pH/GSH-responsive Polyoxometalate Cluster Hybrid Platform for Enhanced Tumor-Specific Phototheranostics. *Angew. Chem. Int. Ed.* 2018;57:14101–14105.
- [21] Donnier-Maréchal M, Septavaux J, Jeamet E, et al. Diastereoselective Synthesis of a Dyn[3]arene with Distinct Binding Behaviors toward Linear Biogenic Polyamines. *Org. Lett.* 2018;20:2420–2423.
- [22] Pappas CG, Mandal PK, Liu B, et al. Emergence of Low-symmetry Foldamers from Single Monomers. *Nat. Chem.* 2020;12:1180–1186.
- [23] Vial L, Ludlow RF, Leclair J, Pérez-Fernández R, Otto S. Controlling the Biological Effects of Spermine Using a Synthetic Receptor. *J. Am. Chem. Soc.* 2006;128:10253–10257.
- [24] Ye Q, Zhu D, Xu L, Lu X, Lu Q. The Fabrication of Helical Fibers with Circularly Polarized Luminescence via Ionic Linkage of Binaphthol and Tetraphenylethylene Derivatives. *J. Mater. Chem. C*. 2016;4:1497–1503.
- [25] Li J, Liu K, Chen H, et al. Functional Built-In Template Directed Siliceous Supramolecular Vesicles as Diagnostics. *ACS Appl. Mater. Interfaces*. 2017;9:21706–21714.
- [26] Qian W, Zuo M, Sun G, et al. The Construction of an AIE-based Controllable Singlet Oxygen Generation System Directed by a Supramolecular Strategy. *Chem. Commun.* 2020;56:7301–7304.
- [27] Chen J, Li S, Wang Z, et al. Synthesis of an AIEgen Functionalized Cucurbit[7]uril for Subcellular Bioimaging and Synergistic Photodynamic Therapy and Supramolecular Chemotherapy. *Chem. Sci.* 2021;12:7727–7734.
- [28] Wu X, Li Y, Lin C, Hu X-Y, Wang L. GSH- and pH-responsive Drug Delivery System Constructed by Water-soluble Pillar[5]arene and Lysine Derivative for Controllable Drug Release. *Chem. Commun.* 2015;51:6832–6835.
- [29] Zhao Y, Shi C, Yang X, et al. pH- and Temperature-sensitive Hydrogel Nanoparticles with Dual Photoluminescence for Bioprobes. *ACS Nano*. 2016;10:5856–5863.
- [30] Zhao H, Sun D, Tang Y, Yao J, Yuan X, Zhang M. Thermo/pH Dual-responsive Core-shell Particles for Apatinib/Doxorubicin Controlled Release: Preparation, Characterization and Biodistribution. *J. Mater. Chem. B*. 2018;6:7621–7633.
- [31] Shang Y, Zheng N, Wang Z. Tetraphenylsilane-cored Star-shaped Polymer Micelles with pH/Redox Dual Response and Active Targeting Function for Drug-controlled Release. *Biomacromolecules*. 2019;20:4602–4610.
- [32] Liu X, Jia K, Wang Y, et al. Dual-Responsive Bola-Type Supra-Amphiphile Constructed from Water-soluble Pillar[5]arene and Naphthalimide-Containing Amphiphile for Intracellular Drug Delivery. *ACS Appl. Mater. Interfaces*. 2017;9:4843–4850.
- [33] Guo D-S, Liu Y. Supramolecular Chemistry of *p*-Sulfonatocalix[n]arenes and Its Biological Applications. *Acc. Chem. Res.* 2014;47:1925–1934.
- [34] Wang Y-X, Zhang Y-M, Liu Y. Photolysis of an Amphiphilic Assembly by Calixarene-Induced Aggregation. *J. Am. Chem. Soc.* 2015;137:4543–4549.
- [35] Wu X, Zhang Y-M, Liu Y. Nanosupramolecular Assembly of Amphiphilic Guest Mediated by Cucurbituril for Doxorubicin Delivery. *RSC Adv.* 2016;6:99729–99734.
- [36] Li P-Y, Chen Y, Chen C-H, Liu Y. Amphiphilic Multi-charged Cyclodextrins and Vitamin K Co-assembly as a Synergistic Coagulant. *Chem. Commun.* 2019;55:11790–21179.
- [37] Hou L, Chen D, Wang R, et al. Transformable Honeycomb-Like Nanoassemblies of Carbon Dots for Regulated Multisite Delivery and Enhanced Antitumor Chemioimmunotherapy. *Angew. Chem. Int. Ed.* 2021;60:6581–6592.